

# Flight Attenuators for the HIFI Local Oscillator Bands

Willem Jellema<sup>1,2\*</sup>, Marcel Bruijn<sup>3</sup>, Jan-Joost Lankwarden<sup>3</sup>, Marcel Ridder<sup>3</sup>, Herman Jacobs<sup>3</sup>, Wolfgang Wild<sup>1,2</sup>, and Stafford Withington<sup>4</sup>

<sup>1</sup>*SRON Netherlands Institute for Space Research, Groningen, the Netherlands*

<sup>2</sup>*University of Groningen, Kapteyn Astronomical Institute, Groningen, the Netherlands*

<sup>3</sup>*SRON Netherlands Institute for Space Research, Utrecht, the Netherlands*

<sup>4</sup>*Cavendish Laboratory, University of Cambridge, JJ Thomson Avenue, Cambridge CB3 0HE, United Kingdom*

\* Contact: W.Jellema@srn.nl, phone +31-50-363 4058

**Abstract**— During the flight instrument level tests of HIFI it became clear that the instrument performance suffered from LO related instabilities. Because the actual LO power requirements of the flight mixers appeared to be an order of magnitude smaller than specified, the LO subsystem was forced to be operated outside its rated and stable operating regime. In order to push the LO power amplifiers back into normal and saturated operation, broadband optical attenuation in all LO bands of around 3 dB up to 18 dB appeared necessary.

In this paper we present the design and development of broadband optical attenuators from first ideas and principles, demonstration, development to space-qualification, flight production, performance characterization and post-delivery to Herschel-HIFI. The as-built attenuators are based on thin Ta films on robust alumina substrates and in a few cases combined with an AR-coating based on a polyimide spinning process. We conclude by presenting the attenuator flight performance, which can be tuned within a few tenths of a dB from target, and essentially provide a flat frequency response from 500 GHz up to more than 2 THz at cryogenic conditions.

## I. INTRODUCTION

At the HIFI Instrument Level Test review (March 13, 2007) system instabilities were reported by J. Kooi [1, 2]. The reported system stability in terms of total power and spectroscopic Allan variance times would seriously affect the scientific observing capabilities of HIFI. This non-conformance situation was followed-up by a detailed investigation by Güsten et al [3]. In their report presented at the HIFI stability meeting on April 3, 2007 it was concluded that a significant contribution to the stability problem could be traced back to the way in which the HIFI Local Oscillators had to be operated so far. It turned out that the input power stage of the LO multiplier chain could not be operated in its rated and stable operating regime. The power amplifiers did not operate in fully saturated mode throughout the HIFI frequency range and inevitably stability problems showed up [4]. The reason behind this unwanted mode of operation was the requirement of continuous frequency coverage. Whereas

in most of the HIFI frequency range the required LO power for the mixers was an order of magnitude lower than available, certain localized areas were known to be problematic in terms of available LO output power due to matching problems inside the multiplier chains. An example of this situation is shown for HIFI band 4 in Fig. 1 where we plot the maximum available LO power measured as a direct detection mixer current.

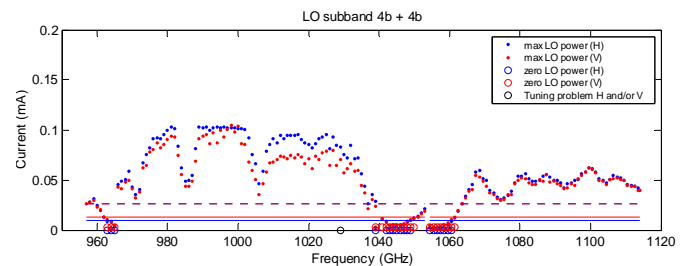


Fig. 1 Maximum available LO power in band 4 (SIS) measured as a direct detection mixer current. The red and blue traces represent the H and V polarizations, the dashed line the optimum mixer current and the solid lines the minimum required currents for H and V resp.

In order to meet the optimum LO power level for the mixers the power amplifiers were forced to operate at very low drain voltage ( $V_d$ ) settings. First of all this operating point creates a strong dependence between the LO power  $P_{LO}$  and  $V_d$ . Because of this large  $\delta P_{LO}/\delta V_d$  ratio the LO power becomes susceptible to bias noise, stability and digital resolution. Since the gain and noise stability of the mixers, especially for the HEB mixers, depend on the LO output power stability, operation near saturated output power settings is favoured. Secondly, operating a power amplifier without significant gain compression can present receiver excess noise because of AM noise sidebands around the LO carrier [4]. Finally the amplifier might become intrinsically unstable at very low drain voltage and problems with stabilization times and hysteresis might occur. Not before evaluation of available ILT test results

at receiver level a system level trade-off had been made to tackle these issues.

A possible recovery for the situation observed for HIFI was proposed by insertion of free-space optical attenuation at the output of the LO. The shift of operating point of the LO system is graphically depicted in Fig. 2. In this diagram the dependence of mixer current versus drain voltage (controlling the input power into the multiplier chain) is shown. By increasing the drain voltages on the power amplifiers the system is put back into saturated output power mode. The mixer current is brought back to a nominal level by the addition of optical attenuation to compensate for excess LO power at higher drain voltages. An additional advantage is the reduction of LO standing waves by increasing the round-trip loss in the LO path [5].

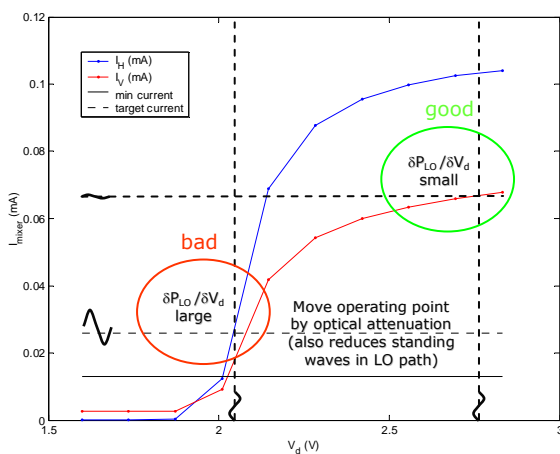


Fig. 2 Schematic diagram illustrating the recovery of receiver stability by bringing the power amplifier back into stable and saturated output power mode by the introduction of optical attenuation.

The tests carried out by Güsten et al confirmed the hypothesis that instable operation of the LO contributes to the receiver stability problem. In [1] Güsten et al show that there exists a distinct transition into stable operating conditions as attenuation and drain voltage of the power amplifier are increased. Now the possible recovery option had been identified, a development and production program for flight attenuators was required.

In this paper we present the results collected to date regarding the development and production of flight attenuators for the HIFI Local Oscillator bands. In this paper we first discuss the technical requirements. Next we present the selected concept, the principle of operation and the implementation of the device in the optical-mechanical design. We present the detailed design of the attenuator device and summarize the characterisation program. We conclude the paper by presenting the production results and measured performance.

## II. TECHNICAL REQUIREMENTS

The general technical requirements that the flight attenuators need to satisfy can be formulated as:

1. Each mixer band shall have its own specific level of attenuation.
2. The range of attenuator values that can be spanned by design shall be -3 to -18 dB
3. The level of attenuation shall be controlled within an accuracy of  $\pm 0.5$  dB
4. The attenuator shall have broadband frequency independent performance with a bandwidth of 200-300 GHz.
5. The attenuator shall operate at an ambient temperature of 130K. The attenuator must withstand temperatures in the range from 100K to 300°C.
6. The attenuator shall be a passive device, no mechanical or electrical control is allowed
7. The attenuator must withstand the acoustic vibration levels applicable to the Herschel satellite
8. The attenuator must be placed external to the Focal Plane Unit outside the Herschel cryostat, and outside of the Local Oscillator Unit box, and be integrated into the baffle assembly containing the de-icing heaters in order to enable replacement if necessary.

Requirements 1 to 4 are driven by the ILT investigations. Requirements 5 to 8 are driven by the thermal and mechanical environment in which the attenuators have to operate. The programmatic constraints for the development and production were tight, a prototype was needed within 2 months for the last phase of ILT prior to delivery, and flight delivery was expected to take place within 3 months.

## III. SELECTED CONCEPT

Initial investigations into the effect of optical attenuation on receiver stability were done at spot frequencies making use of ordinary means of attenuation available in a lab environment. For these tests we used e.g. sandpaper of different granulations, cleanroom paper, black poly-ethylene foils, slabs of Perspex and wire grids. Clearly not all of these solutions can be readily transferred to space application. In order to explore a broad range of possible solutions we structure the various means of optical attenuation, restricted by potential for space application, on the basis of their underlying physical principle:

1. Attenuation by absorption
2. Attenuation by division of polarization
3. Attenuation by reflection

Solutions falling in the 1<sup>st</sup> category, such as high loss tangent dielectrics and carbon loaded polymers, do not offer a feasible implementation. First of all relatively thick slabs of material are required to get attenuation values as large as -18 dB. Moreover anti-reflection coatings are

required to get the associated high frequency Fabry-Perot ripple under control. The frequency dependence is also a problem in terms of a strong slope in the attenuation characteristic across a 200 GHz bandwidth. For a typical attenuator case of -10 dB, the slope can easily become 0.02 dB/GHz. This would correspond to a difference in attenuation of 8 dB between the extremes of the bands we are interested in. Polymers and plastics usually contain large fractions of water contributing to the realized attenuation. As such the attenuation is difficult to control and measure in normal lab conditions. Finally, the use of plastics is not always compatible with the thermal requirements in II.5.

Solutions in the 2<sup>nd</sup> category are also ruled out. Although attenuation by division of polarization, e.g. through wire or planar grids, is a generally accepted means of attenuating a THz signal, it is polarization dependent. Since each LO band is divided up in two subbands, having orthogonal polarization, which are combined through a beam combining grid into a single beam, this solution would only work subband-wise and significantly upset the ratio of delivered power to the H and V polarization channels in each mixer band.

We find that solutions falling in the 3<sup>rd</sup> category appear most promising. Polarization independent devices such as frequency selective surfaces still present a problem in terms of frequency dependence, but partially reflecting surfaces based on lossy thin films are ideal in view of our application. This solution is based on reflecting most of the power (with some residual absorption) at a lossy metallic film and dumping the reflected power in a load. Space-qualified absorbing coatings for such a load are available for and already applied in HIFI [6], The general application of lossy thin films as THz attenuators assumes very thin substrates ( $\ll \lambda/20$ ) to safeguard frequency independent operation and to avoid Fabry-Perot resonances within the substrate over the required frequency band. This is clearly not compatible with our environmental constraints formulated in II.5 and II.7. This complication can be overcome however by a dual-layer design which we will present in the next section of this paper.

IV. PRINCIPLE OF OPERATION

The principle of operation of the selected attenuator option discussed in the previous section is based on partial reflection from and some residual absorption in a lossy metallic film. The lossy film presents an effective surface resistance  $R_s$  and its performance can be simply calculated through a transmission line model consisting only of a shunt admittance  $1/R_s$  matched to the free space impedance [7]. As mentioned earlier the general application consists of a thin metallic film deposited on thin dielectric substrate for mechanical support. An example of the performance of such a device is shown in Fig 3. In this figure it can be seen that the transmittance is -10 dB across the full HIFI frequency range (500 – 1900

GHz). The maximum absorption in a single film is 0.5 or -3 dB, more attenuation is only possible by more reflection and therefore a larger mismatch between the film and free-space.

It is theoretically possible to compose a low-reflectance attenuator by dividing the attenuation over multiple films. An example of such a device is given in Fig. 4. Here we present a 16 layer device with films of 2.6 k $\Omega/\square$  on 3  $\mu\text{m}$  Mylar substrates separated by  $\lambda_0/4$ . The frequency dependence becomes more problematic in the few layer limit, and even with a 16 layer device, which is difficult to manufacture, bandwidth is limited and hard to extend to higher frequencies, also in terms of manufacturing tolerances.

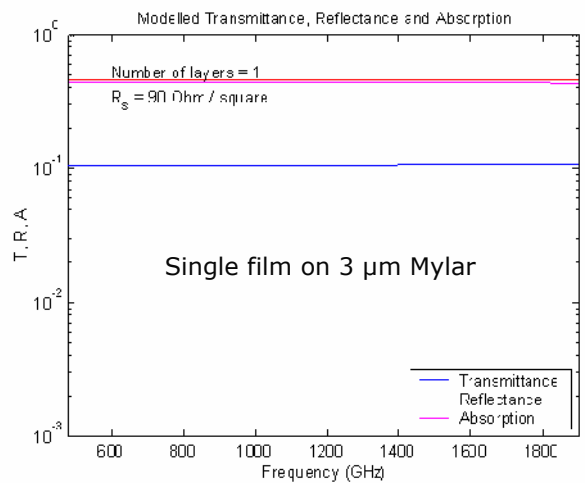


Fig. 3 Frequency independent -10 dB attenuator based on a single film having sheet resistance  $R_s = 90 \Omega/\square$  supported by a 3  $\mu\text{m}$  Mylar substrate.

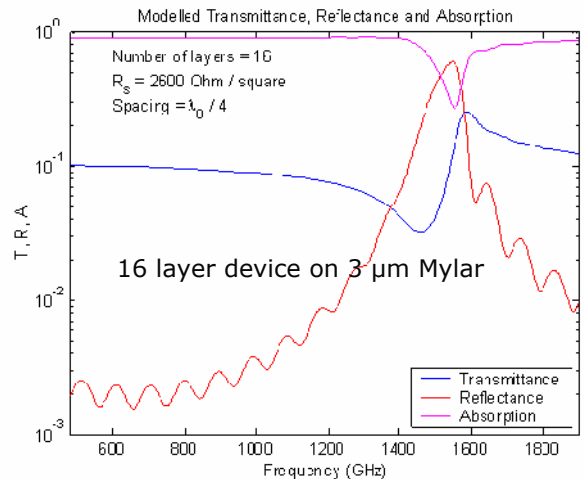


Fig. 4 Multi-layer device with low reflectance composed of 16 lossy films carried on Mylar substrates separated by a quarter-wavelength.

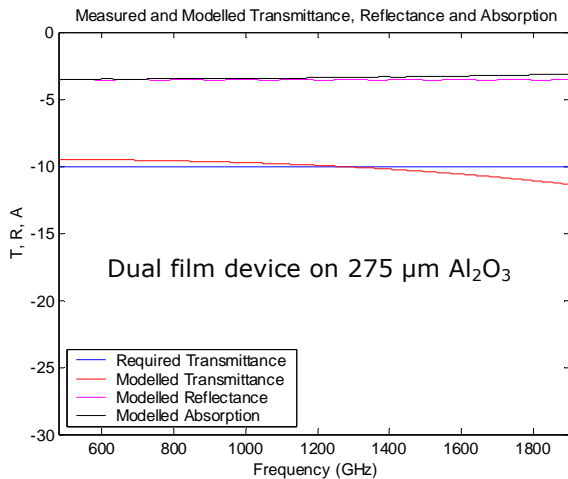


Fig. 5 Dual film device on a relatively thick Al<sub>2</sub>O<sub>3</sub> substrate providing broad-band nearly frequency independent performance.

We select a dual film design in which one film in shunt with free space is impedance matched to the substrate. We refer to this as an impedance matched film. This condition is only met when the sheet resistance  $R_s$  of the film equals  $120\pi / (\sqrt{\epsilon} - 1)$ , where  $\epsilon$  is the dielectric constant of the substrate material. When this condition is met there is zero internal reflection at one face of the Fabry-Perot etalon formed within the substrate. This condition is sufficient to eliminate the Fabry-Perot effect in the substrate and allow for broadband operation only limited by the loss tangent and thickness of the dielectric substrate. Given the impedance matched film, the second layer is chosen in such a way that the additional reflection yields the net total attenuation required. This design is limited in attenuation to -8 dB (reflection and absorption by a single impedance matched film). Between 0 and -8 dB the impedance matched condition can not be met and consequently an AR coating is required to reduce the Fabry-Perot effect. From a mechanical and thermal point of view we select a relatively thick substrate of 0.275 mm of alumina (amorphous sapphire, Al<sub>2</sub>O<sub>3</sub>). For this material we have an in-house Tantalum sputtering process available and it is compliant with the thermal requirement II.5. The material is also compatible with the application of a spin-coated polyimide film as an AR coating. Finally alumina is considered to be a very stable and safe material for space application. An example of a -10 dB attenuator dual-film design is given in Fig. 5. It can be recognized that the Fabry-Perot resonance in the substrate is completely absent, whereas the dielectric loss in the substrate limits the frequency independence.

#### V. OPTICAL-MECHANICAL LAYOUT

The implementation of the dual-film device described before in the optical-mechanical configuration of the LO path is shown in Fig. 6. In this figure the device is tilted by 30° to provide an optical path for the reflected power into the beamdumps. The beamdumps are made of SiC grains embedded in a Stycast glue layer which is qualified for

application on Aluminium. Note that the 30° tilt is a compromise between the volume and space required and a small angle of incidence required to limit polarization dependence of this device. As we explain later the residual polarization effect caused by unequal transmission for the TE and TM cases is used to correct for intrinsic imbalance between the H and V polarization mixers in HIFI by rotation of the device around the optical axis.

The devices are passivated by a SiO<sub>2</sub> coating and then laser-cut to fit within an attenuator holder assembly as shown in Fig. 7. The attenuator holder consists of two Al parts with spiral spring gaskets mounted in three localized slots distributed over the flange. The lids of the laser-cut devices are clamped in between the spiral spring gaskets when the second part of the attenuator holder is mounted on the first. The individual attenuator holders can be mounted on the LO interface plate as shown in Fig. 8. The rotation of individual holders is realized by a periodic hole pattern of 5° in the flange.

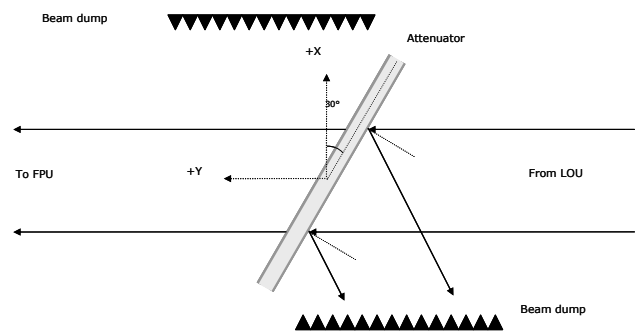


Fig. 6 Dual film attenuator device tilted by 30 deg and surrounded by SiC-Stycast absorber material as a dump.

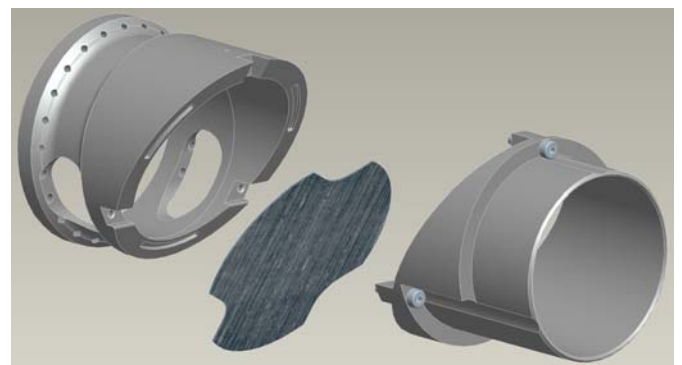


Fig. 7 Laser-cut dual film attenuator clamped in between two Al holder parts.

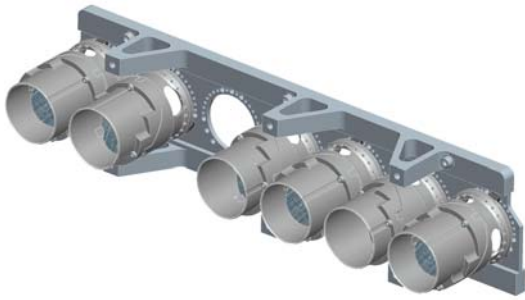


Fig. 8 Attenuator holders mounted on LO interface plate.

### VI. DETAILED ATTENUATOR DESIGN

The individual attenuation required in each mixer band is carefully determined in the ILT configuration by measuring the available LO power distribution across the band versus the drain voltage, a characterization test preceding the  $T_{sys}$  survey reported in [8], and system stability measurements reported in [1, 2]. For verification in ILT we produce a specific test set of attenuators. For flight we also include the expected differences in LO losses between the ILT and spacecraft configurations by individual measurements of the cryostat windows, heat filters, test attenuators and include a margin in a system engineering budget.

The flight attenuation required in each band, the attenuator type and the design parameters are listed in Table 1. For the SIS mixers band 1 to 4 attenuation in the range from -8 to -18 dB is required, whereas the HEB mixers in band 6 and 7 require less attenuation in the range from -3 to -8 dB. Although we target for specific attenuator values, we decide to manufacture attenuator ranges, in 1 dB steps for band 1 to 4 and in 0.5 dB steps for band 6 and 7, to cope with production tolerances and to allow for potential future adjustment. Note that band 5 does not require attenuation. The LO chain for band 5 is already operated at maximum drain voltage and there is no excess LO power.

TABLE III  
ATTENUATOR VALUES AND PARAMETERS IN EACH BAND

Band	Type	Target	$R_s(1)$	$R_s(2)$	$t_{AR}$	Angle
1	dual	-12.2 dB	181 $\Omega/\square$	93 $\Omega/\square$	-	-35°
2	dual	-11.4 dB	181 $\Omega/\square$	112 $\Omega/\square$	-	+60°
3	dual	-9.0 dB	181 $\Omega/\square$	235 $\Omega/\square$	-	-45°
4	dual	-15.7 dB	181 $\Omega/\square$	48 $\Omega/\square$	-	+40°
6	AR	-4.5 dB	257 $\Omega/\square$	-	27 $\mu\text{m}$	0°
7	AR	-3.9 dB	332 $\Omega/\square$	-	24 $\mu\text{m}$	-45°

For band 1 to 4 we adapt a dual-film design. The first Ta layer is a 181  $\Omega/\square$  impedance matched film. The second Ta layer depends on the total attenuation required and is a free parameter to adjust. The  $\text{Al}_2\text{O}_3$  substrates are nominally 275  $\mu\text{m}$  thick and taken from the same batch on which we also calibrate the sheet resistance of Ta versus deposition parameters. Note that the targets and parameters listed apply to ambient conditions in flight. This means that we translate 130K material properties to their equivalents at room-temperature. We come back to this in the next section on characterization results.

For band 6 and 7 the range of attenuation is not compatible with a dual-film design. Here we apply a single high resistivity film and require an AR coating at the other interface. The index of refraction of the alumina substrates we use is 2.09 at 300K. An AR coating of optimum thickness should therefore have an index of refraction of 1.76. Our investigation into materials that are both compliant with the requirements presented in section II and comply with the required index of refraction for the AR coating, shows that Kapton™ or more general polyimide (abbreviated by PI in this paper) provides the closest match. We use an in-house developed process, involving several spin-coating and curing steps, to deposit a PI film of the required thickness on the substrates. The applied AR coatings have an index of refraction of 1.79 and can be controlled at submicron precision.

For both types of attenuator, the dual-film and AR-coated versions, we finally passivate the Ta films by a 0.5  $\mu\text{m}$   $\text{SiO}_2$  passivation layer to avoid ageing of the films.

Using the attenuator test set in the ILT configuration we also determine the polarization dependence empirically by measuring the mixer balance or H/V ratio to ensure balanced delivery of LO power to the mixers. The H/V ratio, which we define as  $(I_H - I_{0H}) / (I_V - I_{0V})$ , where  $I_0$  represent the current without applied LO, is measured as function of rotation angle of the 30° tilted attenuator. An example of the relative gain of mixer current H, being a measure for the coupled LO power, for a given angle of rotation is shown in Fig. 9. In Fig. 9 the relative gain with respect to zero rotation is shown for mixer H and V for LO subbands 2a and 2b in HIFI band 2 at three different frequencies in each LO subband. We use these band dependent empirically determined relative gain characteristics together with the measured available LO power at zero degree rotation with attenuator to calculate the optimum rotation angle for the attenuator. An example of such a calculation is shown in Fig. 10 where the optimized band 1 case is shown. It is clear that the introduction of attenuators allows us to correct for any intrinsic imbalance in the H/V ratio, either due to intrinsic mixer unit differences, alignment differences and/or polarization interface errors. The measured difference in attenuation for the TE and TM cases differs by about 1.5 dB and we find that we can tune the H/V ratio by  $\pm 1$  dB. The rotation angles that result from this exercise and are applicable for flight are also listed in Table I.

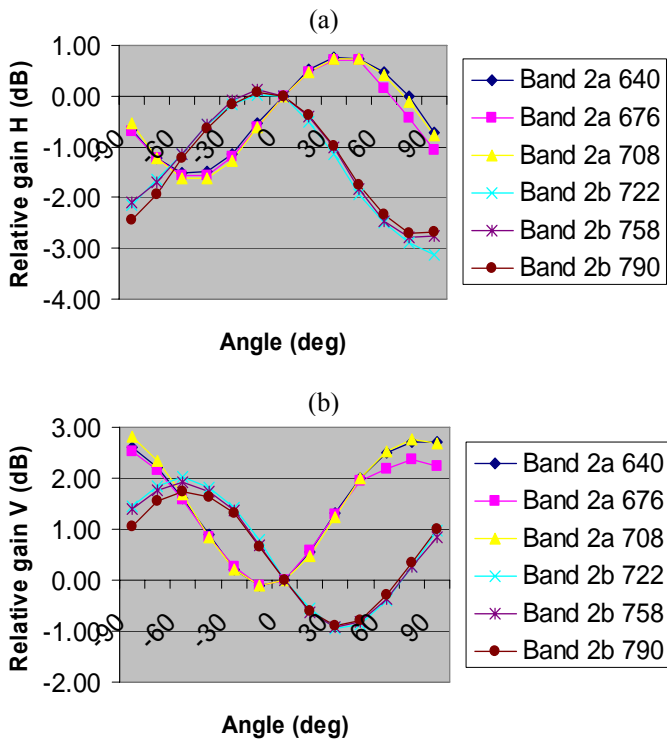


Fig. 9 Relative gain in coupled LO power for mixer H and V as function of rotation around the optical axis for LO subband a and b in HIFI band 2.

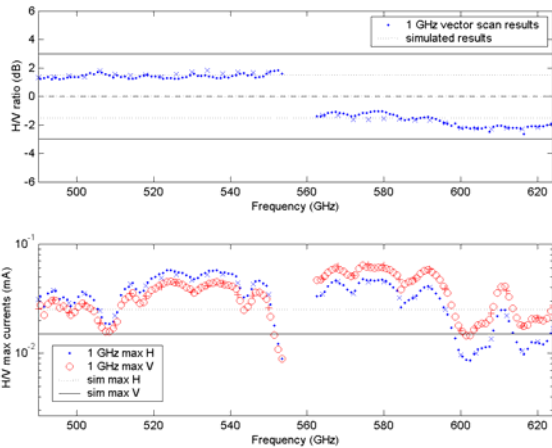


Fig. 10 Measured and simulated H/V ratio and LO power distribution in HIFI band 1. The H/V ratio is optimized by rotation of the attenuators around the optical axis.

### VII. CHARACTERISATION PROGRAM

In this section we summarize the elements of the characterisation program carried out for flight production. The results we summarize both include development tests as well as performance tests on built devices. We do not pretend to be complete here, we will report our final results separately in a journal paper, but like to give the reader an overview of design issues that came across.

#### A. Polarization effects

Since we use the attenuator with an angle of incidence of 30°, there are polarization effects related to differences in the TE and TM reflection coefficients. We include these effects in our modelling and characterisation approach. For transmission and reflection measurements we use a polarized Fourier-Transform Spectroscopy setup in which the samples can be measured at angles of incidence of 0° resp 30° in forward and reverse transmission and reflection. We also measure the state of polarization at the attenuator output by means of measuring the single frequency response in the long-wavelength limit at 625 μm for a 180° scan of an analyser grid in front of a polarized Golay cell as function of angle of incidence of a 45° linearly polarized input beam. We find that for an angle of incidence of 30° the attenuation imbalance for the TE and TM cases is of order 1.5 dB, which is in very good quantitative agreement with the results shown in Fig. 9 and 10.

#### B. Calibration of Al<sub>2</sub>O<sub>3</sub> substrates

The Al<sub>2</sub>O<sub>3</sub> substrates are subject to an extensive calibration campaign. We determine the index of refraction and loss tangent on the basis of model fits to the FTS data obtained for samples of various thickness. The model fit is constrained by precise measurements of the mechanical thickness. We perform measurements and model fits both at room-temperature conditions and as function of temperature and we resolve the complex dielectric constant as function of frequency by assuming a power-law dependence for the loss tangent. Finally we differentiate against the batch of material used. We order large wafer sets to ensure that production of attenuator sets is always carried out on substrates taken from the same batch. A typical example for a specific batch of substrates is shown in Fig. 11. In this figure the temperature dependence of the loss tangent as function of frequency is shown. This data is used in the design model for the attenuators.

#### Temperature dependence tand Al<sub>2</sub>O<sub>3</sub>

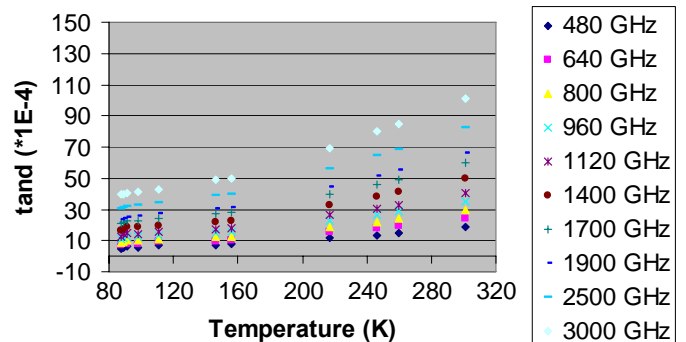


Fig. 11 Loss tangent measurements of Al<sub>2</sub>O<sub>3</sub> versus temperature.

C. Sheet resistance calibration of Ta films

The production of the films is based on an available process at SRON. We deposit Ta films on Al<sub>2</sub>O<sub>3</sub> substrates by RF magnetron sputtering. We make use of an existing calibration of Ta films on polished Si substrates. This calibration establishes a relation between the deposited layer thickness in nm and the RF magnetron power, pressure, exposure time, number of samples in the deposition chamber and the detailed sputtering sequence. Although the translation of measured layer thicknesses in nm on polished Si wafers is awkward and artificial when dealing with unpolished amorphous Al<sub>2</sub>O<sub>3</sub> substrates, we nevertheless use the concept of thickness as an initial parameter to control the process. For each batch of wafers we initially define test structures for DC and RF testing. DC testing is done on Hall bar structures photo-lithographically etched on diced substrates. RF testing is done on 1"x1" diced substrates which are tested in the FTS setup described in A. The RF sheet resistance is determined through a model fit. The DC sheet resistance is determined through a four-point resistivity measurement. Both DC and RF sheet resistances are measured for a range of film thicknesses ranging from 3 to 100 nm at room-temperature and as function of temperature down to 80K.

An example of a room-temperature calibration of R<sub>s</sub> versus film thickness t is shown in Fig. 12. The dashed lines indicated the 2σ error bounds reflecting the production tolerances. The data is fitted to an empirical sheet resistance dependence given by R<sub>s</sub> = R<sub>0</sub> / (t - t<sub>0</sub>), i.e. we assume that there exists an intrinsic oxide layer. This model nicely fits to the data and we find that both the DC and RF sheet resistance agree fairly well within the production tolerances. We find R<sub>0</sub> typically lies in between 2 and 6 kΩnm/□ for substrates taken from different batches. From this we conclude we can use DC diagnostics to control the process and preselect devices.

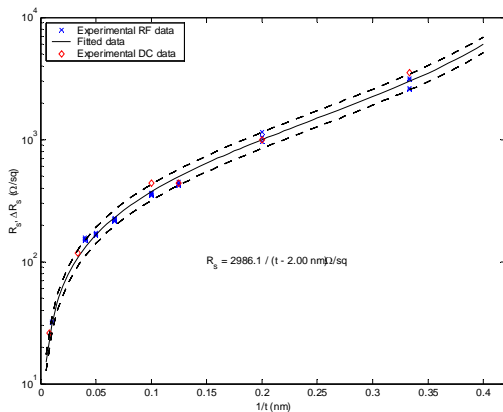


Fig. 12 Example of measured DC and RF sheet resistance as function of film thickness at room-temperature.

The measured dependence of the sheet resistance on temperature is shown in Fig. 13. In this figure it can be

seen that the residual resistivity ratio (RRR) is in general smaller than 1, which implies that the resistivity goes up with temperature and attenuation becomes less due to reduced reflection. This is most visible for the thinner films having R<sub>s</sub> values beyond 200 Ω/□. The thicker films do not show this behaviour and have little temperature dependence. We empirically determine the fractional change of resistance as function of temperature and initial resistance at room-temperature and take this calibration into account in the design. For the attenuator designs presented in Table I the difference in attenuation between room-temperature and 130K is typically within 0.4 - 0.6 dB.

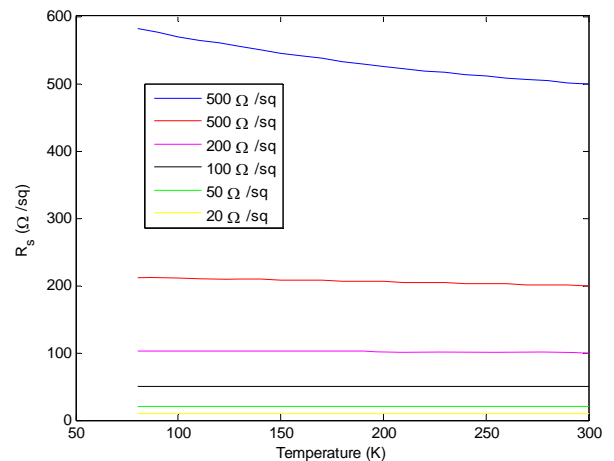


FIG. 13 RELATION BETWEEN SHEET RESISTANCE AND TEMPERATURE.

D. Polyimide Anti-Reflection coating

The polyimide AR coating is applied via a spin-coated process. In this process a polyimide solution is spun on a substrate and then cured. We get best results by building up the total layer thickness by subsequently depositing thinner layers spun at higher spinning rates. The calibration of this process involves measurement of layer thickness after final curing step by a mechanical profiler as function of the curing time and temperature as well as spinning rate. We finally obtain submicron precision in controlling the layer thickness. We also calibrate the dielectric properties as function of frequency and temperature using the FTS procedure described in VII.B for a set of samples with different AR coating thicknesses. An example of measurement results we obtain for a 46 μm thick PI film as function of temperature is shown in Fig. 13. The dielectric losses decrease with decreasing temperature which we taken into account in the design. Using these data and the sheet resistance calibration we design the attenuator sets as shown for example in Fig. 14.

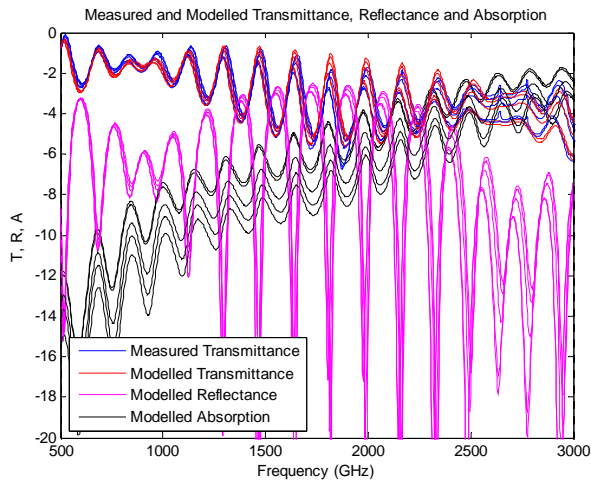


Fig. 13 Example of cryogenic PI film transmission measurements from which we determine the dielectric constant.

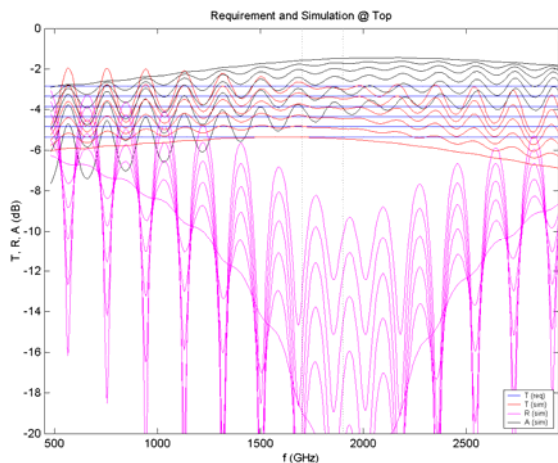


Fig. 14 Attenuator set design for band 7. The PI film thickness is tuned to 1.8 THz and the sheet resistance adjusted to obtain offsets of 0.5 dB in attenuation.

#### E. SiO<sub>2</sub> passivation process

Accelerated life-time tests on bare Ta films at elevated substrate temperatures clearly indicate thermally activated oxidation. We therefore decide to passivate the devices with a 0.5  $\mu\text{m}$  SiO<sub>2</sub> passivation layer. Since the final device is subject to a laser-cut procedure we apply this process immediately after Ta film deposition and in band 6 and 7 before the curing step of the AR coating. We perform dedicated endurance tests as function of time, temperature and relative humidity and conclude that the sheet resistance after passivation and ageing tests remains stable within the accuracy of the experimental facilities. An example of a long endurance test at elevated temperature and humidity is shown in Fig. 15. We do not expect any problems by ageing. In the unlikely event of oxidation prior to launch we only expect an increase of sheet resistance and therefore less attenuation which will not critically affect the HIFI performance in terms of frequency coverage. We also positively confirm that

attenuator performance is not affected by the laser-cutting procedure.

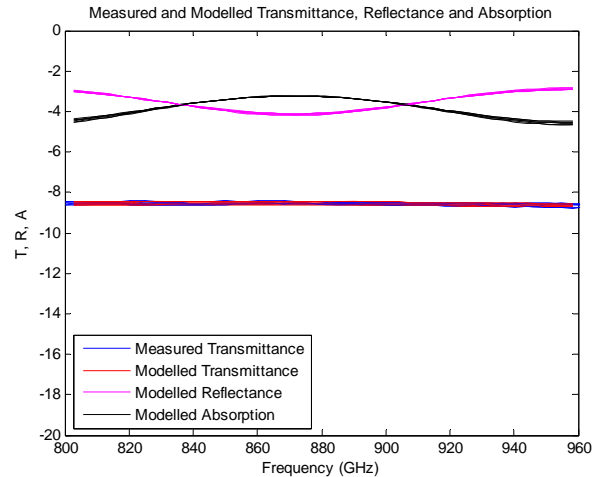


Fig. 15 Endurance test results showing that repeated measurement of sample transmission remains constant over periods of months even when kept at elevated temperatures and high relative humidity.

#### F. PRODUCTION RESULTS AND FINAL PERFORMANCE

In three production runs for band 1 to 4 and two runs for band 6 and 7 we produce 34 potential FM devices for band 1 to 4 and 16 for band 6 and 7. The band 1 to 4 set contains attenuators spanning a range from -7 to -19 dB in roughly 1 dB steps. In band 6 to 7 we achieve a set ranging from -3.5 to -5.0 dB in roughly 0.5 dB steps. Examples of both types of attenuator are given in Fig. 16 resp. 17. In Fig. 18 we also show the attenuator holders.

In Table II we list the flight and spare attenuator values referenced against the target. Note that the P, Q and R stand for a particular substrate batch. We conclude that the measured performance is fully compliant with the target values within the applicable tolerance. Two examples of actual flight attenuator performance are given in Fig. 19 and 20. for a dual-film and AR-coated type respectively.

In Fig. 19 we show the measured performance of P-031 at 300K in blue and the projected performance at 130K in red. The measured transmission is essentially flat across the 500 to 1600 GHz band and within tolerance, indicated by the blue dashed lines  $\pm 0.5$  dB around the target value.

In Fig. 20 the performance of Q-032A is shown. At 1.8 THz it becomes clear that the temperature dependence of dielectric losses in substrate and AR coating need to be taken into account reflected in a difference of almost 1 dB between room-temperature and 130K performance. Furthermore note that the AR coating is properly tuned with a flat region within the 1.7 – 1.9 THz band indicated by the vertical dashed lines. The centre frequency of the AR coating can also be recognized from the dip in the reflectance (purple traces). The projected performance at 130K is compliant with the requirement and falls within the tolerance of  $\pm 0.5$  dB.

The FS devices show nearly identical performance. For band 1 to 4 they correspond to different copies of the same design at different substrates whereas in band 6 and 7 both FM and FS samples are taken from a single larger wafer and are consequently identical within the spread across the wafer.



Fig. 16 Example of a flight attenuator as applied in band 1 to 4.



Fig. 17 Example of a flight attenuator as produced for band 6 and 7.

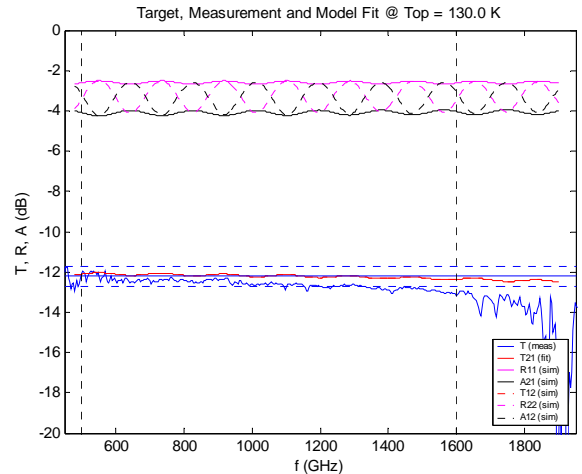


Fig. 19 Measured transmission (blue) and model fit (red) for sample P-031 to be applied in band 2. The horizontal dashed lines indicate the allowed tolerance relative to the target (solid central line).

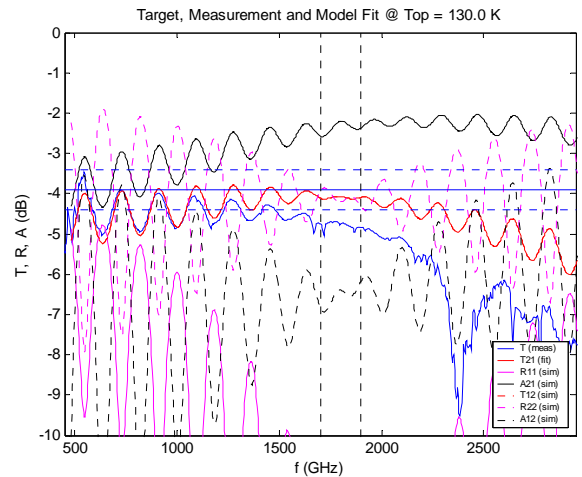


Fig. 20 Transmission measurement results for Q-032A. This device is the FM attenuator for band 7. The vertical dashed lines indicate the required bandwidth. The horizontal blue and dashed lines indicate the target and tolerances resp.

TABLE II  
FLIGHT AND SPARE ATTENUATOR VALUES VERSUS TARGET IN DECIBEL.

Band	Type	Target	FM	Value	FS	Value
1	dual	-12.2	P-033	-12.2	P-034	-12.2
2	dual	-11.4	P-031	-11.3	P-032	-11.5
3	dual	-9.0	P-020	-8.6	P-019	-8.5
4	dual	-15.7	R-031	-15.7	R-035	-15.6
6	AR	-4.5	Q-033A	-4.7	Q-033B	-4.7
7	AR	-3.9	Q-032A	-4.1	Q-032B	-4.1

### SUMMARY AND CONCLUSIONS

In this paper we describe a space-qualified design and production process for broadband THz attenuators or neutral density filters. The attenuators are based on a dual-film concept of lossy metallic films. Broadband operation on substrates as thick as several wavelengths can nevertheless be obtained through an impedance matched film. In our case we deposit thin Ta films on relatively thick Al<sub>2</sub>O<sub>3</sub> substrates and passivate with a SiO<sub>2</sub> layer. This concept works well for attenuator values beyond -8 dB. Between 0 and -8 dB the impedance matched film is replaced by a polyimide AR coating. We achieve excellent agreement between model and measurement and demonstrate flat and broadband performance. The dual film design is extremely broadband and spans the entire HIFI frequency range. For band 6 and 7 we can tune the

thickness of spin-coated AR coatings at submicron precision and successfully align the high frequency bands at THz centre frequencies. The presented design can be tuned to any attenuation value beyond -1 dB and provides space-qualified performance under vacuum and cryogenic conditions.

For HIFI we successfully produce flight and spare attenuator sets fully compliant with the targets set by the project. These devices are currently built into the Herschel spacecraft and are expected to recover from early stability problems encountered during HIFI Instrument Level Testing.

#### ACKNOWLEDGMENT

The authors would like to thank Wim Horinga and Geert Keizer for their considerable effort in testing and characterizing the attenuators. We furthermore recognize the contributions made by Philip Laubert to the laser-cutting process, and Andre van der Horst, Peter Kohsiek and Jaap Evers for procurement and inspection activities as well as general PA/QA support. We finally thank Martin Eggens, Robert Huisman and Jaap Evers for the mechanical design and interface to ESA. All people

mentioned are with SRON Netherlands Institute for Space Research.

#### REFERENCES

- [1] J. Kooi, presentation at HIFI ILT-1 review, March 13, 2007.
- [2] J. Kooi, V. Ossenkopf, M. Olberg, R. Shipman, R. Schieder, and D. Teyssier, "HIFI Stability as Measured During ILT Phase", *these proceedings*
- [3] R. Güsten et al, "HIFI Instabilities – LO-related investigations", HIFI test report MPIfR/HIFI/RP/2007-002, April 6, 2007.
- [4] N. Erickson, "AM noise in drivers for frequency multiplied local oscillators", *Proc. 15<sup>th</sup> Int. Symp. on Space THz Tech.*, April 2004.
- [5] O. Siebertz, C. Honingh, T. Tils, C. Gal, M. Olbrich, R. Bieber, F. Schmuelling and R. Schieder, "The impact of standing waves in the LO path of a heterodyne receiver", *IEEE Trans. Microwave Theory and Techniques*, Vol. 1, No. 12, December 2002.
- [6] M. C. Diez, T. O. Klaassen, C. Smorenburg, K. J. Wildeman, "Reflectance Measurements on Absorbing coating for Sub-Millimeter Radiation", *Proc. 4th Annual Symposium IEEE/LEOS (Benelux Chapter)*, pp. 107-110, 15 November 1999, Mons, Belgium.
- [7] P. F. Goldsmith, "Quasi-optical Systems: Gaussian Beam Quasi-optical Propagation and Applications", IEEE Press: New York, 1997.
- [8] D. Teyssier, N.D. Whyborn, W. Luinge, W. Jellema, J. Kooi, P. Dieleman and T. de Graauw, "HIFI Pre-Launch Calibration Results", *these proceedings*.